Coffman, B. L., Tephly, T. R., Irshaid, Y. M., Green, M. D., Smith, C., Jackson, M. R.., Wooster, R., & Burchell, B. (1990) *Arch. Biochem. Biophys. 281*, 170-175.
Fournel-Gigleux, S., Jackson, M. R., Wooster, R., & Burchell, B. (1989) *FEBS Lett. 243*, 119-122.
Fröhling, W., & Stiehl, A. (1976) *Eur. J. Clin. Invest. 6*, 67-74.
Greenberger, N. J., & Isselbacher, K. J. (1991) in *Harrison's Principles of Internal Medicine* (Wilson, J. D., Braunwald, E., Isselbacher, K. J., Petersdorf, R. G., Martin, J. B., Fauci, A. S., & Root, R. K., Eds.) 12th ed., Vol. 2, Chapter 240, pp 1252-1268, McGraw-Hill, Inc., New York.
Iyanagi, T., Hainu, M., Sogawa, K., Fuji-Kuriyama, Y., Watanabe, S., Shively, J. E., & Anan, K. F. (1986) *J. Biol. Chem. 261*, 15607-15614.
Jackson, M. R., McCarthy, L. R., Harding, D., Wilson, S., Coughtrie, W. H., & Burchell, B. (1987) *Biochem. J.* 242, 581-588.
Kimura, T., & Owens, I. S. (1987) *Eur. J. Biochem. 168*, 515-521.
Mackenzie, P. I. (1990) *J. Biol. Chem. 265*, 3432-3435.
Mackenzie, P. I., Hjelmeland, L. M., & Owens, I. S. (1984) *Arch. Biochem. Biophys. 234*, 487-497.
McKinnon, R. D., Danielson, P., Brow, M. A., Bloom, F. E., & Sutcliffe, J. G. (1987) *Mol. Cell. Biol. 7*, 2148-2154.
Oelberg, D. G., Chari, M. V., Little, J. M., Adcock, E. W., & Lester, R. (1984) *J. Clin. Invest. 73*, 1507-1514.
O'Reilly, D. R., & Miller, L. K. (1989) *Science 245*, 1110-1112.
Parquet, M., Pessah, M., Sacquet, E., Salvat, C., Raizman, A., & Infante, R. (1985) *FEBS Lett. 189*, 183-187.
Parquet, M., Pessah, M., Sacquet, E., Salvat, C., & Raizman, A. (1988) *Eur. J. Biochem. 171*, 329-334.
Radomińska-Pyrek, A., Zimniak, P., Irshaid, Y. M., Lester, R., Tephly, T. R., & Pyrek, J. St. (1987) *J. Clin. Invest. 80*, 234-241.
Ritter, J. K., Sheen, Y. Y., & Owens, I. S. (1990) *J. Biol. Chem. 265*, 7900-7909.
Ritter, J. K., Crawford, J. M., & Owens, I. S. (1991) *J. Biol. Chem. 266*, 1043-1047.
Zimniak, P. Radomińska, A., Zimniak, M., & Lester, R. (1988) *J. Lipid Res. 29*, 183-190.

Interaction of Lysophospholipid/Taurodeoxycholate Submicellar Aggregates with Phospholipid Bilayers†

David G. Shoemaker* and J. Wylie Nichols
Department of Physiology, Emory University School of Medicine, Atlanta, Georgia 30322
Received October 22, 1991; Revised Manuscript Received January 14, 1992

ABSTRACT: The equilibrium partitioning and the rate of transfer of monoacylphosphatidylethanolamines (lysoPEs) between phospholipid bilayers and lysoPE/taurodeoxycholate submicellar aggregates (SMAs) were examined with a series of environment-sensitive fluorescent-labeled *N*-(7-nitro-2,1,3-benzoxadiazol-4-yl)-1-monoacylphosphatidylethanolamine (*N*-NBD-lysoPE) probes of differing acyl chain length. Our previous work has demonstrated the formation of SMAs between bile salts and lysophospholipids [Shoemaker & Nichols (1990) *Biochemistry 29*, 5837-5842]. The experiments in the current work demonstrate that SMAs can coexist with phospholipid vesicles and can function as shuttle carriers for the transfer of lysophospholipids between membranes. The formation of submicellar aggregates of *N*-NBD-lysoPE and taurodeoxycholate (TDC) in equilibrium with 1-palmitoyl-2-oleoylphosphatidylcholine (POPC) vesicles was determined from the increase in fluorescence generated upon addition of TDC to POPC vesicles containing 3 mol % *N*-NBD-lysoPE and 3 mol % *N*-(lissamine rhodamine B sulfonyl)dioleoylphosphatidylethanolamine (*N*-Rh-PE) as a nonextractable fluorescence energy-transfer quencher. The fraction of lysolipid extracted increased as a function of decreasing acyl chain length of the *N*-NBD-lysoPE molecule. The half-time for equilibration was independent of acyl chain length and averaged 44 ms at 10 °C. The delivery of *N*-NBD-lysoPE from preformed *N*-NBD-lysoPE/TDC SMAs into POPC vesicles containing the energy-transfer quencher *N*-Rh-PE was measured by the rate of fluorescence decline. The initial rate of insertion increased with decreasing acyl chain length of the *N*-NBD-lysoPE molecule and as a function of vesicle concentration. The measured rates of *N*-NBD-lysoPE/TDC SMA interaction with vesicles indicate that the dynamic interaction of SMAs with membranes can facilitate intermembrane lysolipid transfer in the presence of nonlytic concentrations of TDC.

The currently accepted role of bile salts in the absorption of phospholipids, cholesterol, fatty acids, and other lipids in the intestine is to solubilize these lipids in mixed micelles that facilitate their transfer through the unstirred water lining the surface of the intestine (Carey et al., 1983; Erlinger, 1987; Wilson, 1981, 1991). Due to the hydrophobic nature of lipids, the unstirred water layer adjacent to the enterocytes of the upper small intestine is the major permeability barrier for their absorption (Wilson et al., 1971; Sallee & Dietschy, 1973; Westergaard & Dietschy, 1974). The amphiphilic structure of bile salts allows them to aggregate with various lipid species in the form of mixed micelles ultimately resulting in the solubilization of large amounts of intestinal lipid (Cabral & Small, 1989). These bile salt/lipid mixed micelles augment

† This study was supported by U.S. Public Health Service Grants GM32342 and DK40641 to J.W.N.
* To whom correspondence should be addressed at Cato Research, Ltd., Suite 201, Westpark Corporate Center, 4364 S. Alston Ave., Durham, NC 27713.

0006-2960/92/0431-3414$03.00/0

lipid absorption by penetrating the unstirred water layer, providing a reservoir for lipids within the unstirred water layer (Westergaard & Dietschy, 1976; Wilson, 1981, 1991). This increases the concentration of these lipid compounds at the bilayer surface and reduces the effective diffusion distance.

Apart from their ability to form mixed micelles above their critical micellar concentration, monomeric bile salts have been shown to interact with hydrophobic molecules, forming submicellar aggregates of unknown stoichiometry with bilirubin IXα (Carey & Koretsky, 1979), cholesterol (Chijiiwa & Nagai, 1989), and lysophospholipid (Shoemaker & Nichols, 1990). Further, submicellar concentrations of bile salts have been demonstrated to accelerate the rate of transfer of phospholipids between phospholipid bilayers (Nichols, 1986). In addition, it has also been shown that the rate of phospholipid movement through the aqueous phase between bile salt/phospholipid mixed micelles is from 200 to 800 times faster than the spontaneous rate between phospholipid vesicles in the absence of bile salts (Nichols, 1988; Fullington et al., 1990). These observations led us to postulate that bile salts could act as shuttle carriers for phospholipids between mixed bile salt/phospholipid micelles, phospholipid vesicles, and the enterocyte membranes in the small intestine. The validity of this working hypothesis depends on the ability of bile salts (1) to form water-soluble complexes with lipids at the low lipid concentrations expected to exist in equilibrium with mixed micelles, phospholipid vesicles, and membranes and (2) to remove and insert lipids from these structures at rates that result in an increase over the spontaneous rate of lipid transfer.

The experiments described in this study employ a model system including lysophospholipids, the bile salt taurodeoxycholate (TDC),[1] and 1-palmitoyl-2-oleoylphosphatidylcholine (POPC) vesicles to test the validity of these two stated conditions. We have used a series of lysophosphatidylethanolamines of differing acyl chain length labeled in the head group with the environment-sensitive fluorescent probe 7-nitro-2,1,3-benzoxadiazol-4-yl (NBD) to study the equilibrium partition levels and the kinetics of these transfer processes. A preliminary report of this work has appeared previously (Shoemaker & Nichols, 1991).

Experimental Procedures

Materials and Routine Procedures. NaTDC was purchased from Sigma Chemical Co., stored desiccated at room temperature, and periodically analyzed for purity by silica gel thin-layer chromatography. Recrystallization was performed when more than one spot on the TLC plate was present after 100 μg of TDC was spotted and run in chloroform/methanol/acetic acid/water, 65/25/2/4, saturated with 35% H_2SO_4 and charred at 150 °C. POPC and monoacyl(lyso)- and diacylPEs were purchased from Avanti Polar Lipids, Inc., and stored at −80 °C. The fluorescent analogues *N*-(lissamine rhodamine B sulfonyl)dioleoylphosphatidylethanolamine (*N*-Rh-PE) and *N*-NBD-labeled monolauroylPE, dilauroylPE, monotridecanoylPE, monomyristoylPE, dimyristoylPE, monopalmitoylPE, and monostearoylPE were synthesized and purified to greater than 99% purity by a previously published procedure (Struck et al., 1981). The concentration of all phospholipids was measured by the method of Ames and Dubin (1960). Sodium chloride and ethylenediaminetetraacetic acid (EDTA) were obtained from J. T. Baker, Inc. NBD-Cl, 4-(2-hydroxyethyl)-1-piperazineethanesulfonic acid (HEPES), and sodium azide were purchased from Sigma Chemical Co. TDC solutions were prepared in HEPES-buffered saline (HBS): 150 mM NaCl, 0.1 mM Na_2EDTA, 0.04% NaN_3, and 10 mM HEPES, pH 7.4 at 25 or 10 °C as indicated.

Vesicle and Submicellar Aggregate (SMA) Preparation. Lipid solutions in $CHCl_3$, containing *N*-NBD-PE and *N*-Rh-PE present at 0–3% when indicated together with 94–100% POPC, were well mixed, dried under N_2, and desiccated for a minimum of 12 h under vacuum at room temperature. Dried lipid films were then resuspended in buffer to yield 1.0 mM total phospholipid. Unilamellar vesicles were prepared using the method of Hope et al. (1985) by extruding the lipid solution 6 times (Lipex Biomembranes, Inc.) through 0.1-μm polycarbonate filters (Nucleopore Corp.). Vesicles were routinely diluted 10–20-fold with HBS for fluorescence experiments. SMAs were prepared by suspension of a dried lipid film of the respective *N*-NBD-lysoPE in a submicellar concentration of TDC dissolved in HBS that provided sufficient fluorescent signal to be monitored (Shoemaker & Nichols, 1990).

Fluorescence and Light-Scattering Measurements. Steady-state fluorescence and slow kinetic experiments were performed on a Perkin Elmer MPF-44E fluorescence spectrophotometer. Fluorescence (excitation 475 nm, 4-nm slit; emission 530 nm, 4-nm slit) and light scattering (90°, 450 nm, 4-nm slit) were measured while the sample was stirred continuously in a thermostatically controlled (25 °C) water-jacketed cuvette. Rapid kinetic experiment ($\leq$1 s) were performed on an SLM 8000C spectrofluorometer equipped with an SLM stopped-flow apparatus. Equal volumes of two sample solutions were mixed, and the fluorescence was monitored [excitation 475 nm (16-nm slit); emission 530 nm (16-nm slit)]. When suspended in HBS or TDC/HBS solutions, the *N*-NBD-lysoPEs were present well below their respective critical micelle concentrations (CMCs) (Shoemaker & Nichols, 1990).

Results

Demonstration of the Coexistence of SMAs and Vesicles. Before we could perform experiments investigating the coexistence of SMAs with vesicles, it was first necessary to determine the concentration of TDC that dissolved a given concentration of POPC vesicles to ensure that we maintained a vesicular system throughout our experimental TDC concentration range. A control experiment for the subsequent coexistence experiments is depicted in Figure 1. We prepared POPC vesicles containing either 3 mol % *N*-NBD-MPE or 3 mol % *N*-NBD-DMPE together with 3 mol % *N*-Rh-PE and mixed them with the concentration of TDC indicated on the abscissa such that the final concentration of POPC was 50 μM. We then monitored the NBD fluorescence and 90° light scattering sequentially. One can see that as the concentration of TDC was raised above 0.5 mM the light-scattering trace began to decline as the mixed TDC/POPC vesicles were converted into mixed TDC/POPC micelles that scattered light to a much lesser degree. At slightly higher concentrations of TDC, the fluorescence values increased, indicating the distance

[1] Abbreviations: CMC, critical micelle concentration; DOPC, dioleoylphosphatidylcholine; HBS, HEPES-buffered saline [150 mM NaCl, 0.1 mM Na_2EDTA, 0.04% NaN_3, and 10 mM 4-(2-hydroxyethyl)-1-piperazineethanesulfonic acid, pH 7.4, at 10 or 25 °C]; NBD, 7-nitro-2,1,3-benzoxadiazol-4-yl; *N*-NBD-lysoPE, *N*-NBD-1-monoacylphosphatidylethanolamine; *N*-NBD-LPE, *N*-NBD-1-monolauroylphosphatidylethanolamine; *N*-NBD-TPE, *N*-NBD-1-monotridecanoylphosphatidylethanolamine; *N*-NBD-MPE, *N*-NBD-1-monomyristoylphosphatidylethanolamine; *N*-NBD-PPE, *N*-NBD-1-monopalmitoylphosphatidylethanolamine; *N*-NBD-SPE, *N*-NBD-1-monostearoylphosphatidylethanolamine; *N*-Rh-PE, *N*-(lissamine rhodamine B sulfonyl)dioleoylphosphatidylethanolamine; POPC, 1-palmitoyl-2-oleoylphosphatidylcholine; TDC, taurodeoxycholate.

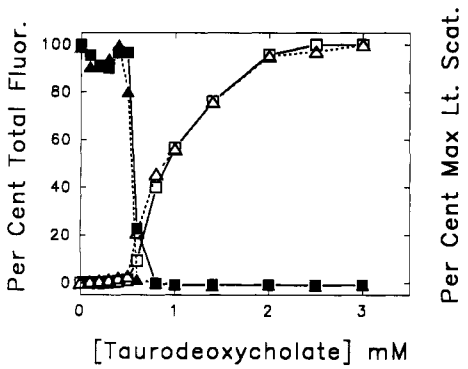

FIGURE 1: Experiment sequentially monitoring the fluorescence (open symbols, excitation 475 nm, slit 4.0 nm; emission 530 nm, slit 4.0 nm) and the 90° light scattering (filled symbols, 450 nm, slit 4.0 nm) of 50 μM POPC vesicles containing either 3 mol % *N*-NBD-MPE (triangles, dotted line) or 3 mol % *N*-NBD-DMPE (squares, solid line) together with 3 mol % *N*-Rh-PE after the addition of the designated concentrations of TDC at 25 °C. The light-scattering decrease was used to indicate the TDC concentration at which the POPC vesicles dissolved into mixed micelles (>0.5 mM). The fluorescence trace in both cases was seen to increase as the TDC dissolved the vesicles containing the energy-transfer pair, thereby increasing the intermolecular distance between the fluorophores.

between the resonance energy-transfer pair *N*-NBD-PE and *N*-Rh-PE had also increased as these molecules were diluted into the mixed micelles. A slight increase in fluorescence at TDC concentrations below 0.5 mM was also noted in the vesicles containing *N*-NBD-MPE but not *N*-NBD-DMPE. We hypothesized that this slight difference in the two fluorescence traces at concentrations below 0.5 mM TDC was a manifestation of the ability of TDC to extract the monoacylated probe *N*-NBD-MPE but not the diacylated probe *N*-NBD-DMPE from the POPC bilayer.

In an attempt to more closely examine the small fluorescence change observed at concentrations of TDC below 0.5 mM, NBD fluorescence was measured following the mixing of equal volumes of POPC vesicles containing 3 mol % *N*-NBD-MPE and 3 mol % diacylated *N*-Rh-PE and buffer containing TDC at high gain in a spectrofluorometer equipped with a stopped-flow apparatus (Figure 2). Progressively more fluorescence was observed as the concentration of TDC was raised from 0 to 0.45 mM. The half-time for equilibration was the same for all concentrations. For these TDC concentrations equal to or below 0.45 mM, the fluorescence increase could be accurately predicted by a single-exponential function. Raising the concentration of TDC to 0.5 mM ≤ [TDC] < 2.0 mM resulted in a slow increase in fluorescence ($t_{1/2} \geq 1$ s) following the initial rapid equilibration. At TDC concentrations of 2.0 mM or greater, a maximal fluorescence level was obtained rapidly ($t_{1/2} \leq 3.4$ ms). At all TDC concentrations, the increase in fluorescence results from the removal of the *N*-NBD-lysoPE from the vicinity of the energy-transfer quencher *N*-Rh-PE. At high TDC concentrations (>0.5 mM), *N*-NBD-lysoPE is separated from the *N*-Rh-PE as a result of dissolution of the vesicles into mixed micelles. However at low TDC concentrations (≤0.45 mM), the increase in fluorescence did not result from vesicle dissolution since no decrease in light scattering was observed in this range (Figure 1).

If one takes the equilibrium level of fluorescence obtained for a trace such as the one in Figure 2 and expresses it as a percent of the total fluorescence obtained upon the mixing of the vesicles with 2.0 mM TDC, one obtains data such as those shown in the upper trace of Figure 3. The observed increase in fluorescence could be due to either TDC extracting the

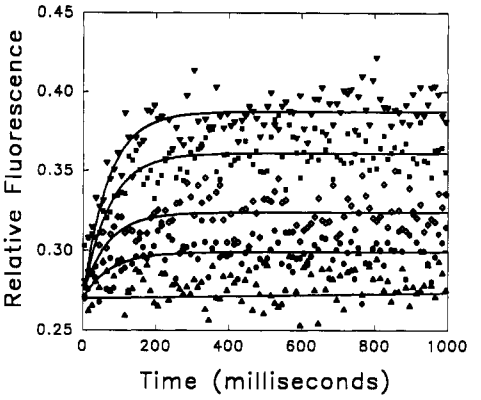

FIGURE 2: Typical records obtained at 10 °C for the time course of the fluorescence increase associated with the extraction of the monoacylated lipid *N*-NBD-MPE from vesicles (3% *N*-NBD-MPE/3% *N*-Rh-PE/94% POPC; final total lipid concentration of 50 μM) upon mixing with increasing concentrations of TDC. Symbol definitions, values for the single-exponential rate constants (k), and equilibrium relative fluorescence values (F_{eq}) were as follows: (△) HBS; (●) 0.1 mM TDC, $k = 13.3 \pm 2.9$ s^{-1}, $F_{eq} = 0.2992 \pm 0.0006$; (◇) 0.2 mM TDC, $k = 14.2 \pm 1.9$ s^{-1}, $F_{eq} = 0.3240 \pm 0.0007$; (■) 0.4 mM TDC, $k = 9.74 \pm 0.94$ s^{-1}, $F_{eq} = 0.3613 \pm 0.0008$; (▽) 0.45 mM TDC, $k = 11.5 \pm 0.8$ s^{-1}, $F_{eq} = 0.3878 \pm 0.0008$. The values for both parameters that gave the best fit of the data are listed ± the standard error for these estimates calculated according to Bevington (1969). Data points shown are the mean of 10 successive time points taken from the averaged records of 5 experimental runs. Solid lines were generated from a single-exponential equation using the parameters obtained from a nonlinear least-squares analysis (Marquardt, 1963) of the averaged data for a given concentration of TDC.

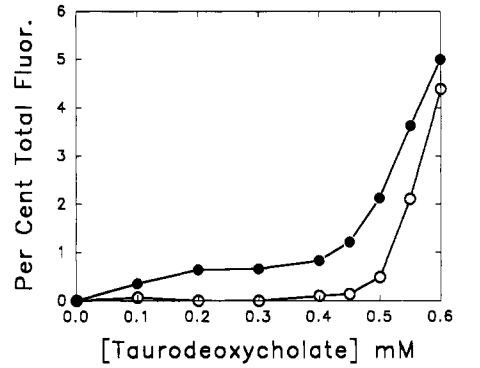

FIGURE 3: Demonstraton of the ability of TDC to extract *N*-NBD-MPE (●) but not *N*-NBD-DMPE from POPC vesicles (○) at 10 °C. The vesicle preparations contained 3% *N*-NBD-MPE or *N*-NBD-DMPE/3% *N*-Rh-PE/94% POPC and were present at a final concentration of 50 μM. The figure is generated from the maximum relative fluorescence values obtained from the traces generated in Figure 2 expressed as the percent of the maximal fluorescence achieved that occurred at 2 mM TDC. The increase in fluorescence that occurred at the higher concentrations of TDC was accompanied by a parallel decrease in light scattering and was presumed to be due to dissolution of the vesicles. Similar results were obtained with the monoacylated and diacylated lauroyl and tridecanoyl derivatives. Fluorescence traces for data points equal to or greater than 0.5 mM TDC did not plateau at steady-state values in 1 s as the lower concentrations in Figure 2, but continued on with a positive slope. Therefore, the data points represent the fluorescence value attained in 1 s.

N-NBD-MPE from the quenching environment of the rhodamine-containing vesicles, resulting in the formation of an SMA, or TDC partitioning into the vesicle bilayer, thereby reducing the resonance energy transfer between the NBD and rhodamine moieties. The increase in fluorescence cannot be attributed to the lysolipid probe leaving the quenching environment of the vesicle and partitioning into the aqueous phase as a monomer because the quantum yield of NBD decreases

by 2 orders of magnitude when transferred from a phospholipid bilayer to an aqueous environment (Nichols, 1987).

To test the second possibility that TDC was partitioning into the bilayer and decreasing the fluorescence energy transfer between the NBD and rhodamine moieties, we employed a diacylated *N*-NBD-DMPE derivative that would be less likely to be extracted from the vesicles upon exposure to TDC. The lack of any observed fluorescence increase in the lower trace of Figure 3 [until the vesicles begin to dissolve ([TDC] ≥0.5 mM)] indicates that the fluorescence increase observed in the upper trace at concentrations ≤0.45 mM was most likely not attributable to TDC partitioning into the phospholipid bilayer and increasing the distance between the NBD and rhodamine. If the increase in fluorescence observed with the monoacylated phospholipid was simply due to the insertion of TDC causing separation of the fluorophores, the DMPE data would be superimposed on the upper trace. The data at concentrations of TDC above 0.45 mM were taken from traces similar to those shown in Figure 2 that exhibited no fluorescence saturation level within the time alotted for recording, so the percent of the maximal fluorescence that was reached in 1 s has been plotted.

One additional explanation for the increase in fluorescence upon addition of the bile salt to vesicles containing *N*-NBD-MPE but not *N*-NBD-DMPE was that the monoacylated *N*-NBD-MPE was in some way altering the lipid packing in the bilayer such that TDC was able to gain access to the bilayer and separate the resonance energy-transfer pairs in a way that was not possible in the vesicles containing only diacylated lipids. To rule out this possibility, we prepared vesicles that contained 3 mol % monomyristoylphosphatidylethanolamine (MPE) in addition to the 3 mol % *N*-NBD-DMPE and 3 mol % *N*-Rh-PE and found that these vesicles gave results that were indistinguishable from the vesicles containing only the *N*-NBD-DMPE and *N*-Rh-PE (data not shown). Therefore, it was not simply the presence of 3 mol % monoacylated lipid in the bilayer that was causing the fluorescence increase we observed in Figures 2 and 3.

Thus, we conclude that the most reasonable interpretation of the fluorescnce increase observed at TDC concentrations below 0.45 mM was the TDC-induced extraction of *N*-NBD-MPE from the quenching environment of the *N*-Rh-PE-containing vesicles into a hydrophobic environment provided by the resulting lysoPE/TDC SMA. The concentration of the two probes in the vesicles was such (3 mol % *N*-NBD-MPE and 3 mol % *N*-Rh-PE) that the fluorescence of the *N*-NBD-MPE was maximally quenched (data not shown). Therefore, any fluorescence change observed could be attributed to the increase in fluorescence of the *N*-NBD-MPE leaving the quenching vesicle environment and not some complex function of an increase in the fluorescence of the *N*-NBD-MPE leaving the vesicle coupled with a decrease in the vesicle fluorescence due to the loss of a submaximally quenched *N*-NBD-MPE molecule.

Acyl Chain Dependence of the Extraction Process. The acyl chain dependence of the extraction of lysoPE derivatives from POPC vesicles by TDC was examined, and the results are shown in Figure 4. As the number of carbons attached to the *N*-NBD-lysoPE was increased (lauroyl < tridecanoyl < myristoyl), the percent of the lysophospholipid extracted from the bilayer was decreased. The relatively more hydrophilic C_{12} lauroyl derivative *N*-NBD-LPE had almost 5% of the total probe extracted from the bilayer by the highest concentration of TDC. Consistent with the degree of extraction being inversely related to hydrophobicity, the diacylated *N*-NBD-

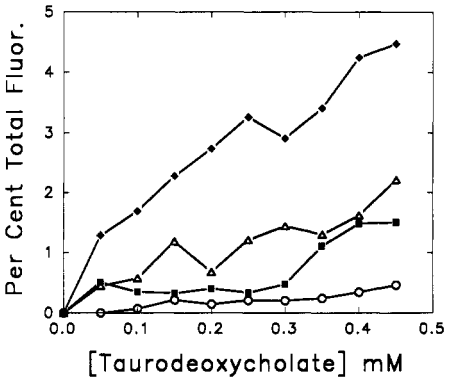

FIGURE 4: Demonstration of the acyl chain dependence of the extraction of *N*-NBD-lysoPE derivatives as a function of TDC concentration at 10 °C. Symbol definitions are (♦) *N*-NBD-LPE, (△) *N*-NBD-TPE, (■) N-NBD-MPE, and (○) *N*-NBD-DLPE. Vesicle preparations were analogous in composition and equal in concentration to those in Figure 3. Percent fluorescence change was calculated as in Figure 3. Note that there was a slight extraction of the diacylated derivative *N*-NBD-DLPE, presumably due to the more hydrophilic nature of this compound relative to the DMPE derivative (Figure 3) that was not extracted to any appreciable extent. The results shown are from one representative experiment.

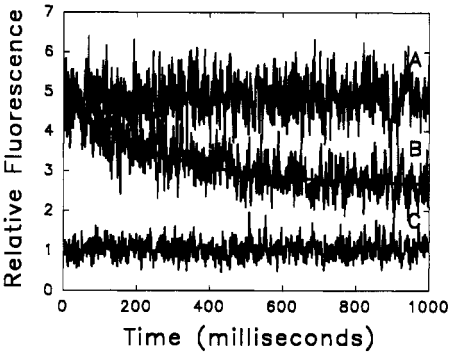

FIGURE 5: Experimental trace demonstrating the delivery of *N*-NBD-PPE from *N*-NBD-PPE/TDC SMAs (0.1 μM *N*-NBD-PPE/0.4 mM TDC) to POPC vesicles (3% *N*-Rh-PE/97% POPC; 50 μM) at 25 °C. Traces represent the fluorescence upon mixing equal volumes of (A) *N*-NBD-PPE/TDC SMAs with HBS, (B) SMAs with 3% *N*-Rh-PE/POPC vesicles, and (C) 3% *N*-Rh-PE/POPC vesicles with HBS. The solid line in trace B was the best fit of the data generated to a single exponential with offset using a nonlinear least-squares regression analysis (Marquardt, 1963).

DLPE began to be extracted to a measurable extent from the bilayer unlike the more hydrophobic *N*-NBD-DMPE (Figure 3). These results indicate that the forces governing the extraction of the lipids mediated by the bile salt, TDC, were primarily determined by the hydrophobic interactions between TDC and the lipids.

Demonstration of the Insertion of LysoPEs by Bile Salts. An investigation of the ability of lysoPE/TDC SMAs to deliver bound lysoPE molecules to phospholipid vesicles was carried out, and representative experimental traces are shown in Figure 5. The uppermost trace (A) depicts the fluorescence resulting from mixing equal volumes of *N*-NBD-PPE/TDC SMAs and HBS. The final concentration of the SMA solution after mixing was 0.1 μM *N*-NBD-PPE and 0.4 mM TDC, in HBS. At these respective concentrations, neither the *N*-NBD-PPE nor the TDC forms simple micelles (Shoemaker & Nichols, 1990). The bottom trace (C) results from mixing equal volumes of 3 mol % *N*-Rh-PE/97 mol % POPC vesicles and HBS (final [vesicles] = 50 μM phospholipid). When equal volumes of this same solution of SMAs and the rhodamine-containing vesicles were mixed (B), the fluorescence of the *N*-NBD-PPE was quenched as the probe moved from the

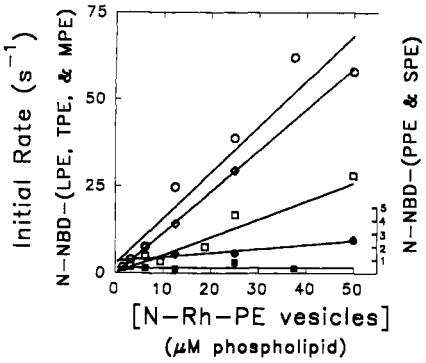

FIGURE 6: Demonstration of the effect of lysolipid acyl chain length on the initial rate of transfer of *N*-NBD-lysoPEs from SMAs to POPC vesicles (3% *N*-Rh-PE/97% POPC) at 25 °C. The data represent a compilation of experiments performed as in Figure 5. The concentrations of the respective SMAs were (■) 0.01 μM *N*-NBD-SPE, (●) 0.1 μM *N*-NBD-PPE, (□) 0.5 μM *N*-NBD-MPE, (○) 0.5 μM *N*-NBD-TPE, and (◇) 0.5 μM *N*-NBD-LPE together with 0.4 mM TDC. Solid lines are generated from linear regression analysis.

SMA complex with TDC to the POPC vesicles. Monitoring the light scattering at this ratio of TDC to POPC assured us that the vesicle integrity was maintained under these conditions (data not shown). The solid line in the decaying trace (B) represents the best fit to a single exponential with offset. The fact that the fluorescence trace (B) does not decay to the constant level of fluorescence maintained by trace C results from the contribution to the fluorescence signal from the probe remaining complexed in the SMAs since the POPC vesicle concentration (50 μM) was not sufficient to extract all of the probe from the TDC (0.4 mM) present in solution.

Acyl Chain Dependence of the Insertion Processes. The effect of varying the acyl chain length of the lysoPE probes on the initial rate of transfer from the SMAs to the vesicles is depicted in Figure 6. The initial rate of transfer was calculated according to the equation:

$$\text{initial rate } (\%/s) = k_{app}(\delta F/\delta F_{max})$$

where k_{app} is the rate constant derived from the best fit of a single exponential with offset to the fluorescence decay in an experiment such as the one depicted in Figure 5 and $\delta F/\delta F_{max}$ is the fraction of the maximal fluorescence change produced by each of the concentrations of POPC vesicles employed. By decreasing the length of the acyl chain from 18 to 13 carbons, we observed a corresponding increase in the initial rate of delivery of lysolipids from the SMAs to the vesicles; however, shortening the chain to 12 carbons resulted in no further acceleration of the rate. We reasoned that this saturation in the initial rate of delivery of the lysolipids resulted from attaining the limit for a diffusion-limited bimolecular reaction occurring in aqueous solution (see Discussion).

Discussion

In order for lysophospholipid/bile salt SMAs to be of physiological significance to lipid transfer between mixed micelles, vesicles, and membranes, they must coexist with these aggregates, and accelerate the rate of lipid exchange over that observed in the absence of bile salts. The results in Figures 3 and 4 showed an increase in fluorescence as low concentrations of TDC are added to POPC vesicles containing *N*-NBD-lysoPEs quenched by *N*-Rh-PE. We interpret these results to indicate the formation of water-soluble complexes of *N*-NBD-lysoPE and TDC in equilibrium with intact POPC vesicles. Our data showed that monoacylated derivatives were extracted to a greater extent than diacylated derivatives and that the extent of extraction of the monoacylated derivatives

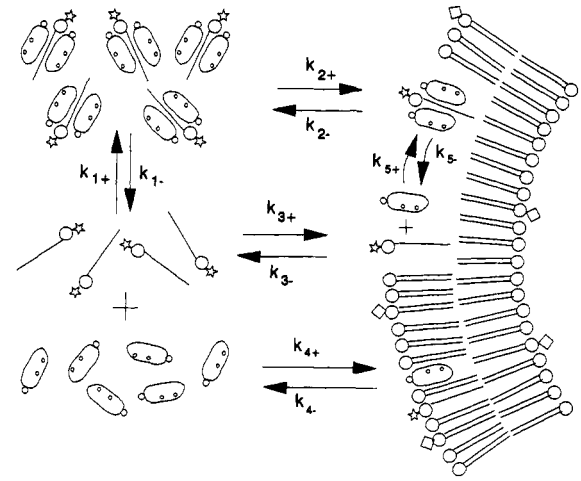

FIGURE 7: Schematic drawing of the molecular species present under the experimental conditions employed in this study. The phospholipid bilayer is meant to represent the artificial vesicles prepared by the extrusion technique in our studies but also could ultimately represent the vesicles known to exist in the bile and intestinal lumen as well as the enterocyte luminal membrane. Phospholipids and lysophospholipids are represented by the traditional ball and stick figures with 18 carbons each on 2 and 1 chain, respectively. The NBD fluorophore attached to the head group of the lysolipids is represented by a star (☆), and the rhodamine attached to the nonextractable diacylated phospholipid is represented by a diamond (◇). The taurodeoxycholate molecule is drawn roughly to scale and is represented by an oval containing the two circular hydroxyl groups with the side chain and taurine represented by a circle on the side of the oval. The SMAs are represented by a single lysolipid complexed with two bile salts for simplicity; however, at the present time, the actual stoichiometry of these submicellar complexes is unknown (Shoemaker & Nichols, 1990).

increased with decreasing acyl chain length. This dependence of the fluorescence increase on the hydrophobicity of the probe argues against it resulting from the interaction of bile salt with the NBD moiety at the vesicle interface. Given that the fluorescence of the NBD probes is highly quenched when they are dissolved in water (Monti, 1977), the most reasonable interpretation of the observed fluorescence increase is that the *N*-NBD-lysoPE probes are removed from the quenching environment of the *N*-Rh-PE vesicles by their hydrophobic association with TDC in the water phase. Simultaneous measurements of the 90° light scattering of the vesicle solution demonstrated that these fluorescence increases occurred at TDC concentrations below those required to dissolve the vesicles.

On the basis of this interpretation, we present a schematic representation of the reactions occurring in our model system (Figure 7). We have measured the rates of extraction for several *N*-NBD-PEs from vesicles during SMA formation (Figure 4) and the rates of their transfer from preformed SMAs into vesicles (Figure 6) in order to determine whether SMAs can function to accelerate lysolipid transfer between phospholipid bilayers. The first-order rate constant for *N*-NBD-MPE removal from 50 μM POPC vesicles by 0.4 mM TDC was measured to be 10 s^{-1} at 10 °C. The first-order rate constant for insertion of *N*-NBD-MPE from SMAs existing in 0.4 mM TDC into 50 μM POPC vesicles was measured to be 26 s^{-1} at 25 °C (Figure 6). Since the first-order rate constants for insertion and removal are similar in magnitude, neither process can be defined as rate limiting, and the overall rate for intervesicular transfer will be in the same range as that for either of the two component steps. Both of these rates are significantly faster than the first-order rate constant for *N*-NBD-MPE transfer between similar concentrations of

phospholipid vesicles (0.5 s^{-1}; unpublished data) measured according to the method of Nichols (1986), and one could conservatively estimate a 50-fold increase in the rate of transfer mediated by SMAs. Therefore, we conclude that SMAs are likely to function as physiological carriers for lysolipids to facilitate their transfer between phospholipid bilayers.

It is experimentally more difficult to demonstrate SMA coexistence with mixed phospholipid/bile salt micelles due to the rapid collision-dependent exchange of lipids between these structures (Nichols, 1988). However, given the higher concentration of soluble bile salt in equilibrium with mixed micelles relative to those in these vesicle experiments, our demonstration of SMA formation in equilibium with vesicles is the more stringent condition. Thus, we predict that SMAs coexist with all lipid aggregates that are in equilibrium with water-soluble bile salts.

The fact that the $t_{1/2}$ for the *N*-NBD-lysoPE extraction process was independent of the TDC concentration despite the increase in the fraction of probe extracted (Figure 2) indicates that the initial rate of extraction was increasing with TDC concentration. This observation was consistent with the rate-limiting step in the formation of SMAs being dependent on the total concentration of TDC. Whether the concentration of TDC of importance is the aqueous or intramembranous concentration has yet to be determined. The accelerated rate observed is presumably due to increasing lysolipid dissociation via some combination of reaction 2- or 3- (Figure 7).

Focusing on the insertion process, in general the shorter the acyl chain of the lysolipid, the more rapidly it was inserted into the bilayer via the SMA (Figure 6). The observation that decreasing the acyl chain length from 13 to 12 carbons failed to accelerate the rate of delivery of lysolipid to the POPC vesicles is most likely due to the fact that the insertion rate has become diffusion-limited. One calculates the rate constant for transfer according to the equation:

$$k\ (M^{-1}\ s^{-1}) = R/([SMA][vesicles])$$

where R = the initial rate of lysolipid insertion (M/s), [SMA] = 0.5 μM, and [vesicles] = 1.25 nM [50 μM phospholipid divided by the estimate of 40 000 phospholipid molecules per 0.1-μm-diameter vesicles (Merrill & Nichols, 1985)]. Taking a value of 60 s^{-1} for the fastest fractional initial rate of insertion for *N*-NBD-TPE (Figure 6), and since the total SMA probe concentration is 0.5 μM, the value for R is 3.0×10^{-5} M/s. Thus, one obtains a value for $k = 4.8 \times 10^{10}\ M^{-1}\ s^{-1}$. This value is in the range of values for a diffusion-limited bimolecular reaction occurring in aqueous media (Gardiner, 1972). Thus, decreasing the acyl chain length of the lysolipid beyond 12 carbons would be unlikely to further accelerate the rate of insertion.

Our measurement of the amount of *N*-NBD-MPE complexed with TDC in equilibrium with POPC vesicles (Figure 3) was greater than that predicted on the basis of the interaction of intervesicular, water-soluble *N*-NBD-MPE and TDC, assuming no bile salt-induced effects on the membrane. For example, from the measured equilibrium constant for the partitioning of *N*-NBD-MPE between DOPC vesicles and aqueous media (5.8×10^5; unpublished data), the concentration of water-soluble *N*-NBD-MPE in equilibrium with vesicles was calculated from $[N\text{-NBD-MPE}]_{total}/(1 + K_{eq}[vesicles])$ to equal 17 nM when $[N\text{-NBD-MPE}]_{total} = 0.5$ μM and [vesicles] = 50 μM. Our previous study (Shoemaker & Nichols, 1990) demonstrated that approximately 3% of the total *N*-NBD-MPE in solution would form SMAs in the presence of 0.4 mM TDC. Therefore, 0.5 nM or 0.1% of the total probe was predicted to form *N*-NBD-MPE/TDC SMAs at the experimental concentrations employed. In fact, the experimental results (Figure 3) show an order of magnitude greater extraction of the *N*-NBD-MPE from POPC vesicles than predicted (1% versus 0.1%). This was most likely due to a bile salt-induced decrease in the equilibrium constant for *N*-NBD-MPE partitioning into the bilayer (Figure 7; reaction 3), resulting in an increase in the *N*-NBD-MPE concentration in the aqueous phase. Both the extraction process and the decrease in the partition coefficient would serve to increase the "effective" aqueous concentration (monomeric and SMA-associated) that is an intermediate in the transfer process.

It should be noted that 0.5 mM TDC was sufficient to dissolve the 50 μM POPC vesicles. This concentration is well below the concentration of TDC necessary to form simple micelles in a pure TDC solution (Kratohvil et al., 1983; Roda et al., 1983) or in solutions containing low concentrations of lysophospholipids (Shoemaker & Nichols, 1990). This is consistent with the observation made in a number of laboratories that the concentration of some bile salts need not reach their respective CMCs to dissolve phospholipid vesicles (Lichtenberg et al., 1979; Schurtenberger et al., 1985; Walter et al., 1992). This supports the concept that some factor other than the aqueous concentration of taurodeoxycholate monomers is a primary determinant of vesicle dissolution (Schurtenberger et al., 1985). Most likely, this determinant is the partitioning of a critical concentration of this bile salt into the phospholipid bilayer (Lichtenberg, 1985).

In the current study, we have demonstrated the ability of the bile salt TDC to extract lysophospholipids from phospholipid bilayers, resulting in the formation of submicellar aggregates that associate primarily on the basis of hydrophobic interactions. We have also demonstrated the ability of these lysophospholipid/TDC SMAs to deliver their associated lysophospholipid to phospholipid bilayers. From our measurements of the time course of these processes, we predict that SMAs function to facilitate the exchange of lipids in the presence of high concentrations of bile salts.

Registry No. POPC, 26853-31-6; TDC, 516-50-7.

References

Ames, B. N., & Dubin, D. T. (1960) *J. Biol. Chem. 253*, 769–775.

Bevington, P. R. (1969) *Data Reduction and Error Analysis for the Physical Sciences*, McGraw-Hill, New York.

Cabral, D. J., & Small, D. M. (1989) in *Handbook of Physiology—The Gastrointestinal System III* (Schultz, S. G., Forte, J. G., & Rauner, B. B., Eds.) pp 621–662, Waverly, New York.

Carey, M. C., & Koretsky, A. P. (1979) *Biochem. J. 179*, 675–689.

Carey, M. C., Small, D. M., & Bliss, C. M. (1983) *Annu. Rev. Physiol. 45*, 651–677.

Chijiiwa, Y., & Nagai, M. (1989) *Biochim. Biophys. Acta 1001*, 111–114.

Erlinger, S. (1987) in *Physiology of the Gastrointestinal Tract* (Johnson, L. R., Ed.) pp 1557–1580, Raven, New York.

Fullington, D. A., Shoemaker, D. G., & Nichols, J. W. (1990) *Biochemistry 29*, 879–886.

Gardiner, W. C. (1972) *Rates and Mechanisms of Chemical Reactions*, W. A. Benjamin, Menlo Park, CA.

Hope, M. J., Bally, M. B., Webb, G., & Cullis, P. R. (1985) *Biochim. Biophys. Acta 812*, 55–65.

Kratohvil, J. P., Hsu, W. P., Jacobs, M. A., Aminabhavi, T. M., & Mukunoki, Y. (1983) *Colloid Polym. Sci. 261*, 781–785.

Lichtenberg, D. (1985) *Biochim. Biophys. Acta 821*, 470–478.

Lichtenberg, D., Zilberman, Y., Greenzaid, P., & Zamir, S. (1979) *Biochemistry 18*, 3517-3525.
Marquardt, D. W. (1963) *J. Soc. Ind. Appl. Math. 11*, 431-441.
Merrill, A. H., Jr., & Nichols, J. W. (1985) in *Phospholipids and Cellular Regulation* (Kuo, J. F., Ed.) pp 61-96, CRC Press, Boca Raton, FL.
Monti, J. A., Christian, S. T., Shaw, W. A., & Finley, W. H. (1977) *Life Sci. 21*, 345-356.
Nichols, J. W. (1986) *Biochemistry 25*, 4596-4601.
Nichols, J. W. (1987) *J. Biol. Chem. 262*, 14172-14177.
Nichols, J. W. (1988) *Biochemistry 27*, 3925-3931.
Roda, A., Hofmann, A., & Mysels, K. J. (1983) *J. Biol. Chem. 258*, 6362-6370.
Sallee, V. L., & Dietschy, J. M. (1973) *J. Lipid Res. 14*, 475-484.
Schurtenberger, P., Mazer, N., & Känzig, W. (1985) *J. Phys. Chem. 89*, 1042-1049.
Shoemaker, D. G., & Nichols, J. W. (1990) *Biochemistry 29*, 5837-5842.
Shoemaker, D. G., & Nichols, J. W. (1991) *Biophys. J. 59*, 629a.
Struck, D. K., Hoekstra, D., & Pagano, R. E. (1981) *Biochemistry 20*, 4093-4099.
Walter, A., Vinson, P. K., Kaplun, A., & Talmon, Y. (1992) *Biophys. J.* (in press).
Westergaard, H., & Dietschy, J. M. (1974) *J. Clin. Invest. 54*, 718-732.
Westergaard, H., & Dietschy, J. M. (1976) *J. Clin. Invest. 58*, 97-108.
Wilson, F. A. (1981) *Am. J. Physiol. 241*, G83-G92.
Wilson, F. A. (1991) in *Handbook of Physiology—The Gastrointestinal System IV* (Schultz, S. G., Forte, J. G., & Rauner, B. B., Eds.) pp 389-404, Waverly, New York.
Wilson, F. A., & Dietschy, J. M. (1971) *Gastroenterolgy 61*, 911-931.

Interaction of Troponin C and Troponin C Fragments with Troponin I and the Troponin I Inhibitory Peptide†

C. A. Swenson* and R. S. Fredricksen
Department of Biochemistry, University of Iowa, Iowa City, Iowa 52242
Received October 16, 1991; Revised Manuscript Received December 23, 1991

ABSTRACT: We have quantitated the interactions of two rabbit skeletal troponin C fragments with troponin I and the troponin I inhibitory peptide. The calcium binding properties of the fragments and the ability of the fragments to exert control in the regulated actomyosin ATPase assay have also been studied. The N- and C-terminal divalent metal binding domains of rabbit skeletal troponin C, residues 1-97 and residues 98-159, respectively, were prepared by specific cleavage at cysteine-98 and separation by gel exclusion chromatography. Both of the troponin C fragments bind calcium. The calcium affinity of the weak sites within the N-terminal fragment is about an order of magnitude greater than is reported for these sites in troponin C, suggesting interaction between the calcium-saturated strong sites and the weak sites. Stoichiometric binding (1:1) of the troponin I inhibitory peptide to each fragment and to troponin C increased the calcium affinities of the fragments and troponin C. Complex formation was detected by fluorescence quenching or enhancement using dansyl-labeled troponin C (and fragments) or tryptophan-labeled troponin I inhibitory peptide. The troponin C fragments bind to troponin I with 1:1 stoichiometry and approximately equal affinities (1.6×10^6 M^{-1}) which are decreased 4-fold in the presence of magnesium versus calcium. These calcium effects are much smaller than is observed for troponin C. The summed free energies for the binding of the troponin C fragments to troponin I are much larger than the free energy of binding troponin C. This suggests a large positive interaction free energy for troponin C binding to troponin I relative to the fragments. The tryptophan-labeled troponin I inhibitory peptide binds to troponin C and to the N- and C-terminal fragments of troponin C in the presence of calcium with a stoichiometry of 1:1 and association constants of 5.3×10^5, 2.5×10^5, and 6.5×10^4 M^{-1}, respectively. The calcium dependencies of the association constants are largest for troponin C (~10-fold) with smaller values for the N-terminal (~3-fold) and C-terminal (~2-fold) fragments. These data are most easily understood in terms of a solution structure for troponin C which is compact relative to the crystal. The large calcium dependence in the troponin C-troponin I interaction (>50-fold) might arise from the coupling of a conformational change in the N-terminal domain of troponin C with the release of a positive free energy of interaction between the calcium binding domains.

Regulation of the contraction of skeletal muscle is achieved through the dependence of the interactions of the troponin-tropomyosin-actin complex of the thin filament on the presence of calcium ion in the calcium regulatory sites of troponin C (Leavis & Gergely, 1984). An understanding of the molecular basis of this regulation is contingent on a knowledge of the structures and interactions of all the protein components. Structural information is available for troponin C (Herzberg & James, 1985; Sundarlingham et al., 1985), tropomyosin (Caspar et al., 1969; Phillips et al., 1980), and actin (Suck et al., 1981; Engelman & DeRosier, 1983; Kabsch & Holmes, 1990). Although little detailed structural information is known

† This work was supported in part by the American Heart Association.

0006-2960/92/0431-3420$03.00/0